

NUMERICAL SIMULATION OF GMA WELDING - INFLUENCE OF METAL VAPOUR –

Authors: M., HERTEL, U., FÜSSEL, M., SCHNICK
Workplace: Technical University of Dresden, Germany

Abstract:

Current numerical models of GMAW try to combine MHD models of the arc and VoF models of metal transfer. They neglect vaporization and assume an argon atmosphere for the arc region as it is common practice for models of gas tungsten arc welding. These models predict maximum temperatures of more than 20,000 K and a temperature distribution similar to TIG arcs. However, current spectroscopic temperature measurements in GMA arcs demonstrate much lower arc temperatures. In contrast to TIG arcs they found a central local minimum of the radial temperature distribution.

This paper presents a GMA arc model that considers the formation of metal vapour on the one hand and its influence on the arc characteristics on the other hand. An axial-symmetric model of the work piece, the wire and the arc is used. MHD as well as turbulent mixing and thermal demixing of metal vapour in argon are included. The results are in very good agreement with experimentally observed temperatures and temperature distributions. The model is able to predict the local central minimum in the radial temperature and the radial electric current density distributions.

1. INTRODUCTION

In GMAW processes the arc is burning between the continuously leading wire and the workpiece. The properties of the arc and its attachment at the electrode determine the material transfer. On the other hand the arc approach and arc properties are influenced by the electrode geometry, the temperature, the current density and the vaporization of the electrodes. Comprehensive process understandings as well as a temporal and regional high resolution of the physical process parameters are necessary to minimize the experimental effort and to enable a precise development of GMAW processes with an increased process capability, less emission and enhanced fields of application.

In the past different complex numerical models were developed to illustrate the complex cause-and-effect-chain and to develop welding processes [1] [2]. The former GMAW models are all LTE-one component fluids of argon or helium. Based on the work of LOWKE [3] the arc approach at the electrodes is modelled by using a coarse grid with an element height of about 0.5 mm. SPILLE-KOHOFF [4] simulates MIG impulse arcs by using a finer grid at the electrodes and the sheath model of LOWKE [5] and SANSONNES [6]. All referred workings evaluate the arcs with profiles of temperature and fluid flow which were determined experimental and numerical for TIG arcs. Directly below the wire the maximum calculated temperatures of the arc column are between 20,000 K and 23,000 K. The highest radial temperatures can be assigned to the arc column and are almost over the whole arc length 16,000 K.

Spectroscopic investigations on impulse arcs [7] [8] show the important influence of the process gas on the one hand and of the metal vaporization during the impulse phase on the composition of the plasma of GMAW arcs on the other hand. The vaporization of the wire material is the reason for the metal vapour dominated arc core in the impulse phase. Additionally the maximum arc temperature and the particle density of electrons and ions

Charge conservation

$$\text{div} \vec{j} = 0 \quad (1) \quad \vec{j} \quad \text{Electric current density}$$

Ohm's law

$$\vec{j} = -\sigma \text{grad} \Phi \quad (2) \quad \sigma \quad \text{Electric conductivity}$$

Magnetic potential

$$\text{div} \left(\text{grad} \vec{A} \right) = -\mu_0 \vec{j} \quad (3) \quad \Phi \quad \text{Electric potential}$$

Magnetic field

$$\vec{B} = \text{rot} \vec{A} \quad (4) \quad \vec{A} \quad \text{Magnetic vector potential}$$

The influence of the Lorentz force on the velocity field is considered by a source term in the momentum equations.

Lorentz force

$$\vec{f}_L = \vec{j} \times \vec{B} \quad (5)$$

The resistive heating is regarded by a source term in the energy conservation equation.

Resistive heating

$$S_{RH} = \frac{j^2}{\sigma} \quad (6)$$

The LTE model of [3] is used to calculate the arc attachment at the electrodes. This allows noticeable less computation time because the complex sheath mechanism according to [5] [6] is not considered.

2.2 Plasma properties

The plasma properties have important influence on the GMAW process parameters. Besides the pressure and temperature dependence, the fraction of the metal vapour inside the plasma is considered. In this paper material properties of mixtures of argon and iron vapour from MURPHY [9] are used. Figure 2 shows the influence of the iron vapour on the plasma properties. The plasma radiation is simplified by the net emission model. The net emission coefficient (NEC) of argon and iron is defined as a function of the temperature. The datasets of MENART [10] are used. The net emission coefficient of the argon iron mixture is calculated as follow:

$$NEC_{Mix} = X_{Ar} NEC_{Ar} + X_{Fe} NEC_{Fe} \quad (7)$$

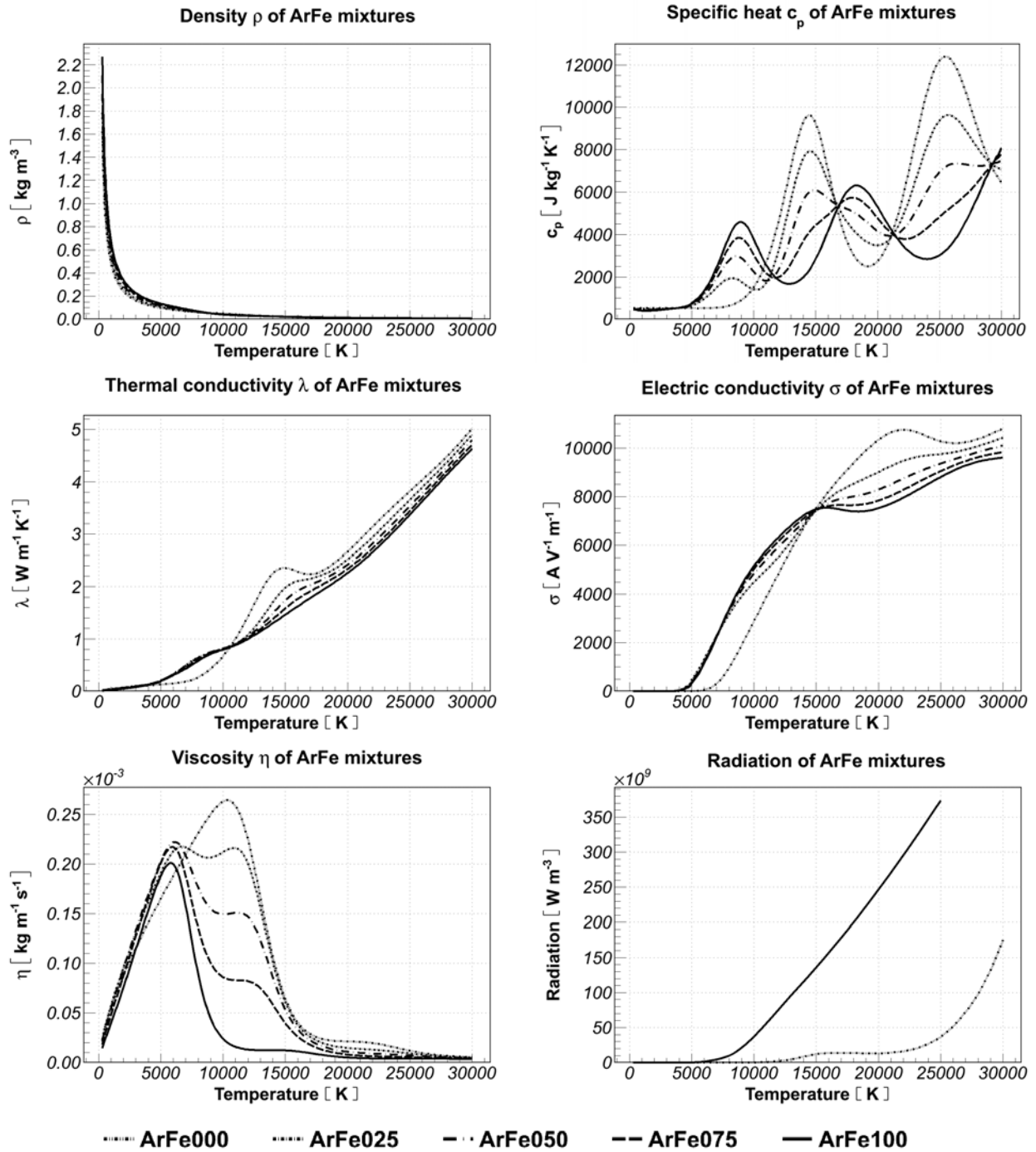


Figure 2 Properties of argon iron mixtures as a function of the molar fraction of iron [9] [10]

2.3 Diffusion and demixing

Diffusion is a physical process which leads to a uniform distribution of particles. But FRIE [11] indicated also the appearance of demixing effects in particular in thermal plasmas due to the high gradients of concentration, temperature, pressure and electric field strength. In this paper the simplified formulation of MURPHY [9] is used.

Argon transport equation

$$\frac{\partial (\rho Y_{Ar})}{\partial t} + \text{div} \left(\rho \vec{u} Y_{Ar} + \vec{J}_{Ar} \right) = 0 \quad (8)$$

with the mass flux

$$\vec{J}_{Ar} = \frac{n^2}{\rho} \bar{m}_{Ar} \bar{m}_{Fe} (D_{ArFe}^X \text{grad } X_{Fe} + D_{ArFe}^p \text{grad } \ln p_{tot} + D_{ArFe}^E \vec{E} - D_{ArFe}^T \text{grad } \ln T)$$

n Number Density

ρ Density of the mixture

Y_{Ar} Mass fraction of argon

t Time

$\bar{m}_{Ar,Fe}$ Molar mass of argon and iron

T Temperature

p_{tot} Total pressure

\vec{E} Electric field

X_{Fe} Molar fraction of iron

$D_{ArFe}^{X,p,E,T}$ Transport coefficients due to gradients in X_{Fe} , p , \vec{E} and T

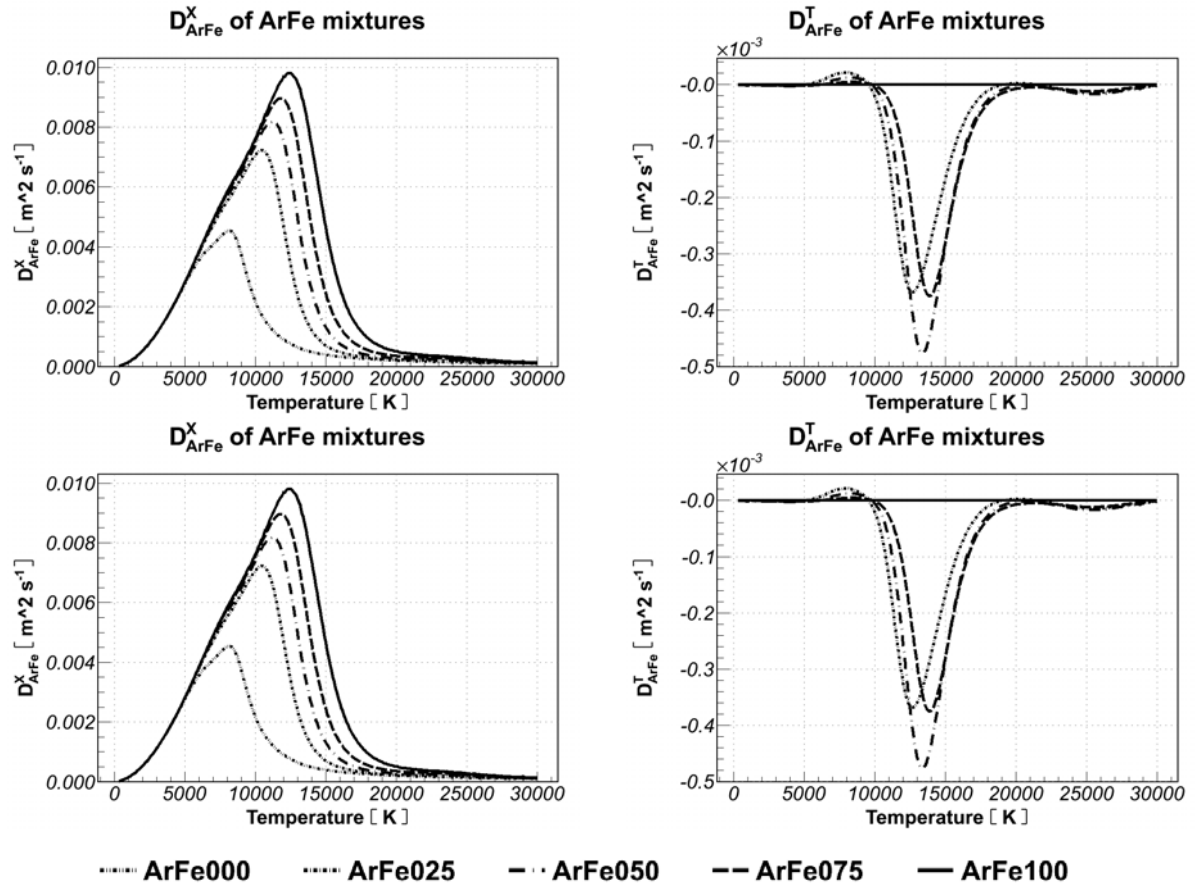


Figure 3 Transport properties of argon iron mixtures [9]

2.4 Vaporization

In a GMAW process the metal vapour is mainly formed by the vaporization of the wire material. Two different possibilities to model the formation of metal vapour are discussed. In the first step a fixed vaporization mass flux of 0.01 %, 0.1 % and 1 % which is referenced on the wire feed is assumed. Therefore an additional, numerical stable analysis of the influence of metal vapour is possible [15].

In a second step the vaporization is implemented self consistently by the specification of the mass concentration of the metal vapour Y_{Fe} at the surface of the electrode IB, see figure 1,[12].

$$Y_{Fe}(T) = \frac{1}{1 + \frac{(p - X_{Fe} p_S(T)) \bar{m}_{Ar}}{X_{Fe} p_S(T) \bar{m}_{Fe}}} \quad (9)$$

$p_S(T)$ Partial pressure of iron as a function of the wire temperature
 p absolute pressure

2.5 Boundary conditions

Argon is used as shielding gas in the calculation domain ABCDEFG, see Table 1. The wire diameter is 1.6 mm; the wire and arc length are 5 mm respectively. For the self consistent formulation of the metal vapour formation a fixed geometry for the droplet is specified.

Table 1: Boundary Conditions

	mass & momentum	energy equation	electric potential	magnetic potential	mass fraction iron vapour
AB	-	T = 300K	$\Phi = 12V$	$\frac{\partial A_i}{\partial n} = 0$	-
BC	$\dot{V} = 15 \frac{l}{min}$	T = 300K	$\frac{\partial \Phi}{\partial n} = 0$	$\frac{\partial A_i}{\partial n} = 0$	$Y_{Fe} = 0$
CD	p = 1atm	T = 300K	$\frac{\partial \Phi}{\partial n} = 0$	$\frac{\partial A_i}{\partial n} = 0$	$Y_{Fe} = 0$
DE	p = 1atm	T = 300K	$\frac{\partial \Phi}{\partial n} = 0$	$A_i = 0$	$Y_{Fe} = 0$
EF	-	T = 300K	$\frac{\partial \Phi}{\partial n} = 0$	$A_i = 0$	-
FG	-	T = 300K	$\Phi = 0V$	$\frac{\partial A_i}{\partial n} = 0$	-
GH	-	$\frac{\partial T}{\partial n} = 0$	$\frac{\partial \Phi}{\partial n} = 0$	$\frac{\partial A_i}{\partial n} = 0$	-
HI	$\frac{\partial \vec{u}}{\partial n} = 0$	$\frac{\partial T}{\partial n} = 0$	$\frac{\partial \Phi}{\partial n} = 0$	$\frac{\partial A_i}{\partial n} = 0$	$\frac{\partial Y_{Fe}}{\partial n} = 0$
IA	-	$\frac{\partial T}{\partial n} = 0$	$\frac{\partial \Phi}{\partial n} = 0$	$\frac{\partial A_i}{\partial n} = 0$	-
IB	$\vec{u} = 0$	-	-	$\frac{\partial A_i}{\partial n} = 0$	Eq.(8)

3. RESULTS AND DISCUSSION

In the first step a fixed metal vapour mass flux relative to the wire feed is assumed. The cooling effect of the wire feed is included simplified by an increased thermal conductivity.

Figure 4 shows the calculated plasma temperature, the metal vapour concentration and the plasma flow for a welding current of 250 A and a vaporization rate of 1 % of the wire feed.

The simulation results correlate with the measurements on GMAW arcs concerning the temperatures as well as the temperature distribution [7],[8],[13]. The plasma temperatures in the core of the arc are characterized by a local minimum of the radial distribution. A good correlation is also achieved for the metal vapour concentration. These results support the sharp-cut limitation of the metal vapour core, which was described by HERMANN [14] and measured by METZKE [7]. In the intermediate layer between the arc core and the arc border area exist a local concentration minimum of metal vapour. This demixing effect is mainly driven by high temperature gradients.

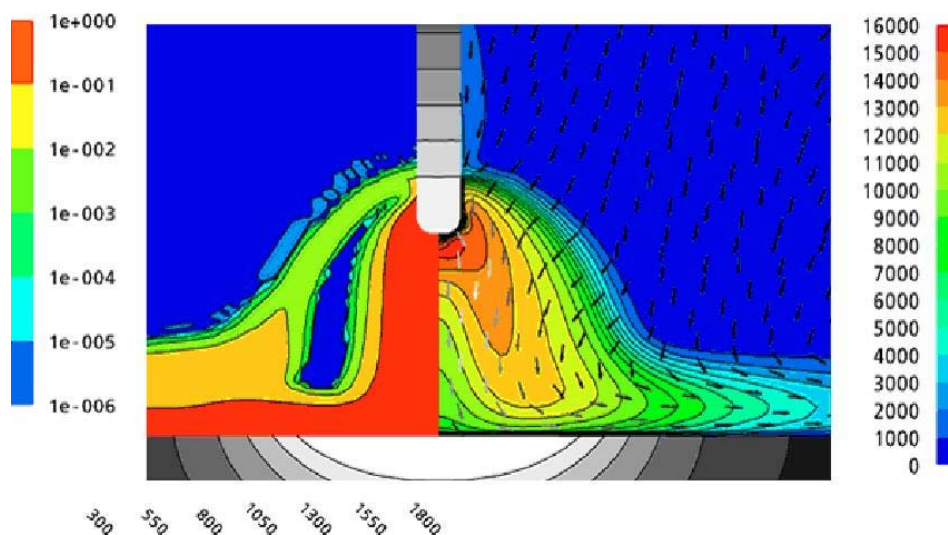


Figure 4 Temperature, arc plasma velocity and iron mass fraction distribution in a 250 A arc with a wire vaporization rate of 1 % of the wire feed

A previous analysis of the particular properties of the metal vapour and their effects on the plasma shows the reason for the minimum in the radial temperature distribution [15]. This effect is caused by the intensive cooling of the arc core due to the high radiation emission of the metal vapour. The calculation shows that the influence of the higher electric conductivity at temperatures below 10,000 K has a lower impact in contrast to the cooling.

In the second step a self consistent formulation of the metal vaporization is used, see figure 5. The arc core is dominated by the metal vapour with a radial temperature minimum. Qualitatively the results of the self consistent model are in good agreement with the results of the fixed metal vapour mass flux model from the first step.

The complex definition of the energy flux on the wire surface is numerically challenging. Additionally to the energy input by the electrons, the cooling by the wire feed, the convective heat flux and the cooling due to the vaporization have to be considered. The

numerical problems have not been solved completely yet, but first sensitive studies show the dominant influence of the energy input by the electrons and the cooling by the wire feed.

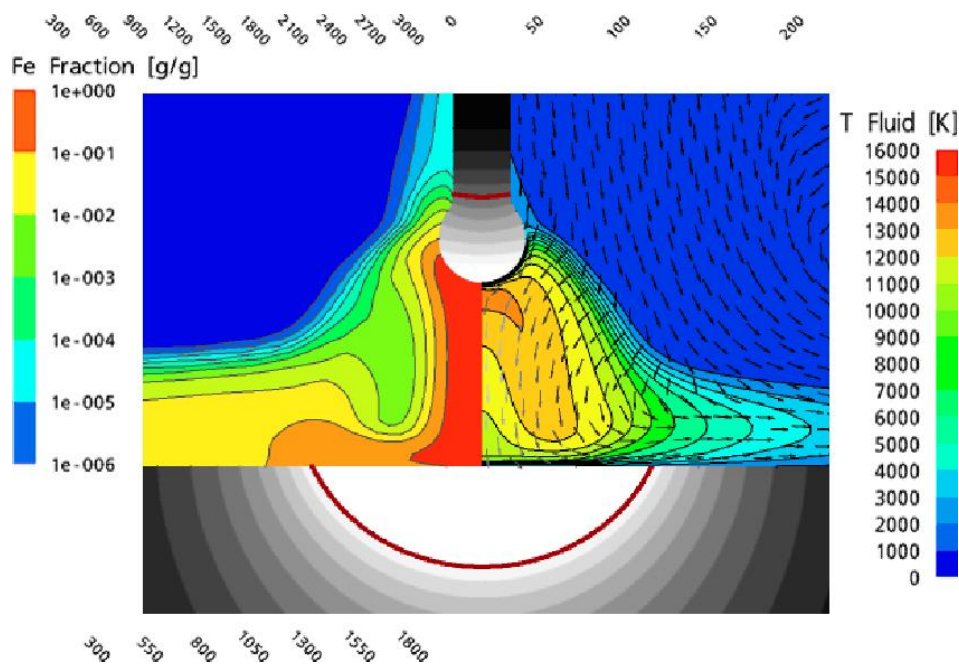


Figure 5 Temperature, arc plasma velocity and iron mass fraction distribution in a 250 A arc with a self consistent wire vaporization rate (according to 0.8 % of the wire feed)

4. CONCLUSION

The two presented GMAW models enable the numerical description of the characteristic temperature distribution in GMAW which was already identified by spectroscopic methods experimentally. With these models effects of thermal demixing can also be considered. Two different possibilities of the definition of the metal vapour mass flux are presented: a fixed metal vapour mass flux model and a self consistent mass flux model. In both the intensive cooling of the arc core due to the high radiation emission is the main reason of the temperature minimum. In the future, the reabsorption inside the optical dense metal vapour will be regarded because of the substitution of the NEC-model by a radiation transport model. Furthermore it is planned to use the calculated surface properties and flows at the intersections of the arc and the electrodes as boundary conditions of the sheath models. With the help of these models the electron and ion current density at the work piece will be calculated.

Acknowledgments

This work was supported by the DFG (FU 307/5-1). The presented results are part of the DFG promoted research project "Erweiterung des Prozessverständnisses über MSG-Lichtbogenprozesse durch Modellierung und Visualisierung der physikalischen Zusammenhänge" ('Enlargement of the process understanding about GMA-arc processes with the help of modelling and visualization of the physical background') as well as of the AiF-DFG-cluster project 'Lichtbogenschweißen - Physik und Werkzeug' ('Arc welding - Physics and Tool').

References

- [1] RADAJ, D. *Schweißprozesssimulation: Grundlagen und Anwendung*. Verlag für Schweißen und verwandte Verfahren DVS-Verlag GmbH, Düsseldorf 1999.
- [2] SCHNICK, M., FÜSSEL, U., SPILLE-KOHOFF, A. *Lichtbogenprozesssimulation von Plasmalichtbögen mit ANSYS CFX 10*. 25th CADFEM User's Meeting, Dresden, 2007
- [3] LOWKE, J. J., TANAKA, M. 'LTE-diffusion approximation' for arc calculations. J. Phys. D: Appl. Phys., Vol. 39, pp. 3634 - 3643, 2006
- [4] SPILLE-KOHOFF, A. *Numerische Simulation des ChopArc-Schweißprozesses*. Abschlussbericht ChopArc, Fraunhofer IRB Verlag, 2005.
- [5] LOWKE, J. J., MORROW, R., HAIDAR, J. A simplified unified theory of arcs and their electrodes. J. Phys. D: Appl. Phys., Vol. 30, pp. 2033 - 2042, 1997.
- [6] SANSONNENS, L., HAIDAR, J., LOWKE J., J. Prediction of properties of free burning arcs including effects of ambipolar diffusion. J. Phys. D: Appl. Phys., Vol. 33, pp. 148 - 157, 2000.
- [7] METZKE, E., SCHÖPP, H. *Spektralanalyse des Metall-Lichtbogenplasmas*. Abschlußbericht ChopArc, Fraunhofer IRB Verlag, 2005.
- [8] GOECKE, S.-F. *Auswirkungen von Aktivgaszumischungen im vpm-Bereich zu Argon auf das MIG-Impulsschweißen von Aluminium*. Dissertationsschrift TU Berlin, 2004.
- [9] MURPHY, A., B. *Thermal plasmas in gas mixtures (Topical Review)*. J. Phys. D: Appl. Phys., Vol. 34, pp. 151 - 173, 2001.
- [10] MENART, J., MALIK, S. Net emission coefficients for argon-iron thermal plasmas. J. Phys. D: Appl. Phys., Vol. 35, pp. 867 - 874, 2002.
- [11] FRIE, W. Entmischungseffekte bei Gemischen ionisierender Atomgase. Zeitschrift für Physik 172, 99-117, 1963.
- [12] YAMAMOTO, K., TANAKA, M. Numerical Simulation of metal vapour behaviour in arc plasma. Surface & Coatings Technology Vol. 202, pp. 5302 - 5305, 2008.
- [13] BRIAND, F. et al. Experimental investigations of the arc in MIG-MAG welding. SG 212, IIW Doc.212-1123-08, Proc. of IIW Meeting, 2008.
- [14] YUDODIBROTO, B. Y. B., HERMANS, M. J. M., DEN OUDEN, G., RICHARDSON, I. M. Observations on Droplet and Arc Behaviour during Pulsed GMAW. SG 212, IIW Doc. 212-1125-08, Proc. of IIW Meeting, 2008.
- [15] SCHNICK, M., FÜSSEL, M., HÄBLER, M., HERTEL, M. *Numerical Investigations of the Influence of Metal Vapour in GMA Welding*. Dresdner Fügetechnisches Kolloquium 2008, Selbstverlag der Technischen Universität Dresden, ISBN 978-3-86780-115-7